

Inhomogeneous electronic states of $\text{La}_{2-x}\text{Sr}_x\text{CuO}_4$ probed by scanning tunneling spectroscopy

T. Kato,* S. Okitsu, and H. Sakata

Department of Physics, Tokyo University of Science, 1-3 Kagurazaka, Shinjuku-ku, Tokyo 162-8601, Japan

(Received 15 July 2005; published 24 October 2005)

Low-temperature scanning tunneling microscopy and spectroscopy have been performed on an optimally doped $\text{La}_{1.84}\text{Sr}_{0.16}\text{CuO}_4$ single crystal at 4.2 K. The surface topography and the spatial variation of the local density of states have been obtained on the ab plane. Our results reveal a nonuniform distribution of low-energy electronic states and the superconducting gap in real space. The energy gap Δ evolves on the surface in the length scale of 5–10 nm, and ranges from 7 to 17 meV. The mean value of $\Delta \approx 10$ meV, which gives $2\Delta/k_B T_c \approx 6$, is in agreement with the previous results of tunneling and angle-resolved photoemission spectroscopy study. The spectra exhibit similar evolution to that of $\text{Bi}_2\text{Sr}_2\text{CaCu}_2\text{O}_{8+\delta}$, suggesting that the electronic inhomogeneity is a common characteristic among high- T_c cuprates. This spatial distribution of Δ in our observation accords with the results of the ^{63}Cu NQR study when it is attributed to the variation of the local hole concentration.

DOI: 10.1103/PhysRevB.72.144518

PACS number(s): 74.25.Jb, 74.50.+r, 74.72.Dn

Scanning tunneling spectroscopy (STS) using a scanning tunneling microscope (STM) provides direct mapping of the local density of states (LDOS) in real space. This technique has been used to investigate the stimulating local electronic states in conventional and high-temperature superconductors (HTS), such as impurity scattering^{1,2} and vortex core states.^{3–9} One of the recent key issues in high-temperature superconductivity is the static electronic inhomogeneity probed by STM/STS in $\text{Bi}_2\text{Sr}_2\text{CaCu}_2\text{O}_{8+\delta}$ (Bi2212).^{10–12} The tunneling spectrum changes from a spectrum with clear coherence peaks, consistent with the $d_{x^2-y^2}$ superconductivity, to the “pseudogaplike” spectrum characterized by a broad spectral feature without apparent coherence peaks on the microscopic length scale close to the superconducting coherence length. This result suggests the coexistence of the hole-rich and hole-depleted regions within the CuO_2 layer. The origin of this nonuniform nature has been explained by electronic phase separation, which is inherent in strongly correlated materials with low carrier density. If this inhomogeneous nature is an intrinsic property of HTS, the various experimental results and theories based on uniform LDOS should be reconsidered. On the other hand, Loram *et al.* maintained that such a gross inhomogeneity exists only on the outermost CuO_2 layer and is not the bulk nature.¹³ It is also claimed that inhomogeneity is critically affected by the sample preparation¹⁴ since hole doping in Bi2212 is achieved by adding extra oxygen atoms. In order to clarify the inhomogeneous nature in HTS, further investigations into the other cuprates is needed.

$\text{La}_{2-x}\text{Sr}_x\text{CuO}_4$ (LSCO) consists of a simple layered perovskite structure with a single CuO_2 layer, and is a typical prototype of the doped Mott-Hubbard insulator. In contrast to Bi2212, hole doping is achieved by the substitution of Sr^{2+} for La^{3+} ; hence, LSCO contains a little amount of oxygen deficiency or excess oxygen, which may affect the inhomogeneity. Therefore, LSCO is a good candidate to elucidate whether or not the inhomogeneity is a general feature on HTS. Singer *et al.* reported the inhomogeneity in LSCO by the ^{63}Cu NQR experiments.¹⁵ From the frequency dependence of the $1/T_1$ curves, they estimated the spatial variation

of the local hole concentration and the “patch” size. The Josephson plasmon resonance and the neutron diffraction experiments have also indicated the existence of the inhomogeneity in LSCO,^{16,17} although the degrees of inhomogeneity do not agree with each other. A few STM/STS experiments in LSCO have been reported.^{18–20} None of them, however, have revealed the surface topography and spatial variation of the tunneling spectra since the surface preparation is difficult in LSCO. Although LSCO does not have as good cleavage as does Bi2212, we have found that the atomically flat surface can be exposed by cleaving the single crystal at a low temperature because of the layered structure in LSCO.²¹

In this paper we report the results of the first genuine STS experiments on the optimally doped LSCO at 4.2 K, and demonstrate the existence of the inhomogeneous superconducting states on the surface. We adopted the conversion of the energy gap into the local hole concentration and found agreement with the results of the ^{63}Cu NQR study.

An optimally doped single crystal was grown by a traveling-solvent floating-zone technique.²² The actual Sr concentration x was determined to be 0.16 by inductively coupled plasma mass spectrometry and electron-probe microscope analysis. The samples for the STM/STS experiments were shaped into cuboids with typical dimensions of $1.0 \times 1.0 \times 3.0$ mm³. The long side was exactly parallel to the c axis, as determined by the Laue method. The samples were annealed in air at 900 °C for 50 h then 500 °C for 50 h to remove the thermal stresses formed during the crystal growth. The superconducting transition temperature T_c was found to be 38 K from SQUID magnetization measurements.

The STM and STS measurements reported here were carried out by a laboratory-built STM at 4.2 K.⁴ The sample mounted in the STM was cleaved (mechanically fractured perpendicular to the c axis) prior to the measurements at 4.2 K in helium gas in order to prepare a clean and fresh surface for the measurements. The prepared surface was flat and almost parallel to the ab plane when the surface was observed by an optical microscope. The bias voltage was applied to the sample, namely, the negative and positive bias correspond to the occupied and unoccupied states, respec-

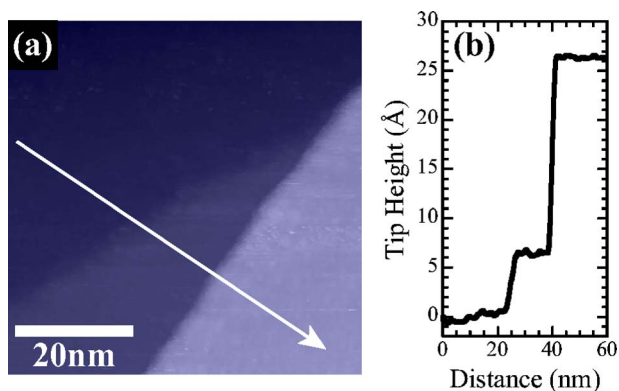


FIG. 1. (Color online) (a) Typical topographic image ($60 \text{ nm} \times 60 \text{ nm}$) taken on the surface of a LSCO single crystal. (b) Cross section along the arrow shown in (a) indicating that the unit of the step height is $c_0/2 \approx 6.6 \text{ \AA}$.

tively. Electrochemically etched Pt-Ir wire was used as a STM tip. The STM/STS measurements were performed in the constant current mode. In the STM observations, large tip-surface spacing was taken to prevent surface degradation by the scanning tip: the typical tunneling parameters were tunneling current $I=0.03 \text{ nA}$ and sample bias voltage $V=300 \text{ mV}$, giving a tunneling conductance of $G=0.1 \text{ nS}$. In the STS measurements the current-voltage (I - V) characteristics were obtained at 64×64 points on the surface. Tunneling spectra, i.e., dI/dV vs V curves, were calculated by numerical differentiation of the measured I - V curves. For the sake of achieving a high signal to noise ratio, G was increased to 2 – 3 nS during STS measurements. Since the tip is perpendicular to the ab plane, the tunneling spectrum primarily represents an angular average of the LDOS over the ab plane. The measurements were performed within two days after the preparation of the surface in order to avoid being influenced by deterioration of the surface quality.

Figure 1(a) shows a typical topographic image of the prepared surface at 4.2 K . Although LSCO has no cleavage, step-terrace structures reflecting a layered structure have been observed. The surface of the terrace is flat, with an overall roughness of less than $1 \text{ \AA}_{\text{p-p}}$. A cross section across the steps shown in Fig. 1(b) indicates that the unit of the step height is approximately 6.6 \AA , which corresponds to $c_0/2$, where c_0 is the lattice constant along the c axis. Thus, the terraces are believed to be parallel to the ab plane. Considering the rigidity of the octahedron in the unit cell, the top-most layer seems to be a LaO layer. A similar situation has been reported in Sr_2RuO_4 ,²³ which has the same K_2NiF_4 structure as LSCO. All the spectra reported in this paper were measured on a terrace, as shown in Fig. 1(a).

Before discussing the evolution of the LDOS on the surface, we show some representatives of the tunneling spectra at 4.2 K in Fig. 2 in order to survey the typical characteristics of the spectra. The asymmetric V-shaped background conductance, with a higher value at a negative bias, is a common characteristic in these spectra. This V-shaped background conductance continued to $\pm 500 \text{ meV}$, which is the maximum range of the bias voltage swept in our measurements. On the degraded sample surface, merely V-shaped

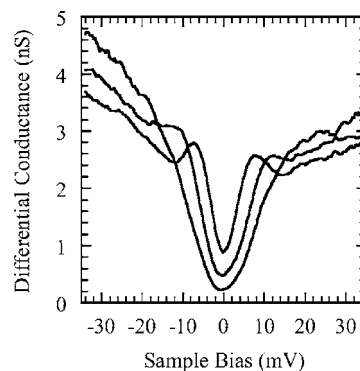


FIG. 2. Representative tunneling spectra of $\text{La}_{1.84}\text{Sr}_{0.16}\text{CuO}_4$ at 4.2 K obtained at different locations on a surface.

spectra with no apparent gap feature were observed. The value of the energy gap Δ and the height of the coherence peaks varied with location. The spectrum having smaller Δ shows the apparent coherence peaks, though the height is not as conspicuous as that of Bi2212. They almost vanish in the spectrum with larger Δ . The zero-bias conductance (ZBC) tends to decline as Δ increases. These variations in the spectra were independent of structural details of the surface topography. Previous reports, including early tunneling studies on polycrystalline samples, exhibit each type of the spectra in Fig. 2.^{18,19}

To demonstrate how the spectra are evolved on a surface we show the results of a STS measurement as a Δ map ($40 \text{ nm} \times 32 \text{ nm}$), with spatial resolution of about 6 \AA in Fig. 3(a). Here, Δ is defined as follows: if the coherence peaks are well defined, the energy separation between the peaks at the positive and negative bias is set to 2Δ . If the coherence peaks are not apparent, the energy difference between the two shoulders, where the second derivative of the tunneling spectrum shows the negative peak, is regarded as 2Δ . The map clearly indicates the existence of the inhomogeneity in Δ , ranging from 7 to 17 meV in real space. The characteristic length scale of the Δ variation is about 5 – 10 nm , which is comparable to the superconducting coherence length $\xi_0 \approx 3$ – 4 nm .²⁴ No characteristic pattern with a particular periodicity or orientation is observed in the Δ map within this resolution. The observed nonuniform distribution is really static in comparison with the results of neutron scattering or NQR experiments, since our STS measurement took about $4 \times 10^3 \text{ s}$ to obtain one LDOS map. Figure 3(b) shows the LDOS evolution taken along the line AB depicted in Fig. 3(a). Both the spectral shape and Δ vary continuously from location to location. Smaller Δ is associated with apparent coherence peaks and large ZBC. This tendency is in agreement with the results of inhomogeneous Bi2212.^{10,11} However, there are discrepancies: over 70% of the spectra have no apparent peaks in LSCO, and the coherence peaks, if they exist, have a much lower magnitude than those in Bi2212.

Figure 4 displays the histogram analysis of the distribution of Δ obtained from the STS measurement shown in Fig. 3. The value of Δ distributes from 7 to 17 meV with the mean value of 10.3 meV , and a full width at half-maximum of 4.2 meV . Because of the broad nature of the spectra at a larger Δ region, Δ above 13 meV is slightly ambiguous. The

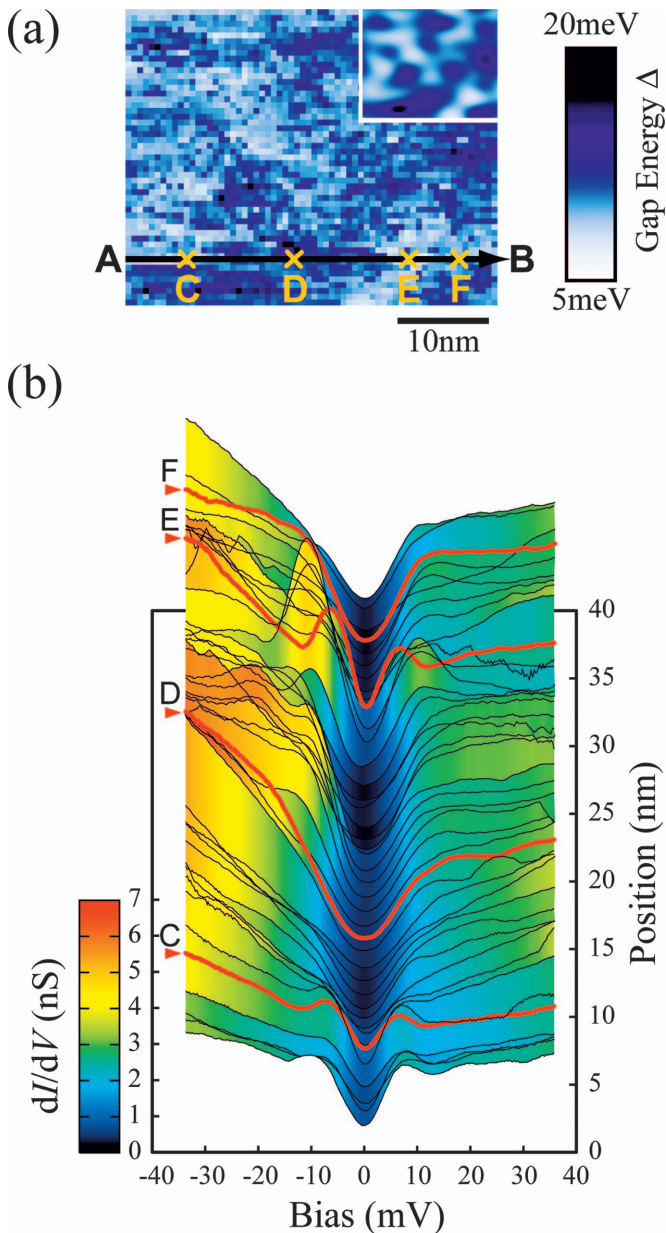


FIG. 3. (Color) (a) Gap map ($40 \text{ nm} \times 32 \text{ nm}$) deduced from the STS experiment at 4.2 K . A brighter color represents a smaller Δ , which corresponds to a higher local carrier density (see Fig. 4). A demagnified low-pass filtered image of whole $40 \text{ nm} \times 32 \text{ nm}$ field of view is shown in the inset to clarify the inhomogeneity of Δ discussed in the text. (b) Line scan of tunneling spectra extracted along the line AB. Some typical spectra drawn in red correspond to the locations indicated by C-F in (a).

mean value of $\Delta \approx 10 \text{ meV}$ in optimally doped LSCO is in agreement with the previous results of the tunneling²⁰ and ARPES²⁵ studies. Since Δ symmetrically distributes around 10 meV corresponding to the optimum doping, it is unlikely that the oxygen deficiency caused by the surface preparation altered the carrier concentration on the exposed surface.

Though the origin of this distribution of Δ is not clear at present, we suppose that it is attributed to the variation in the local carrier concentration p since there is a general trend for

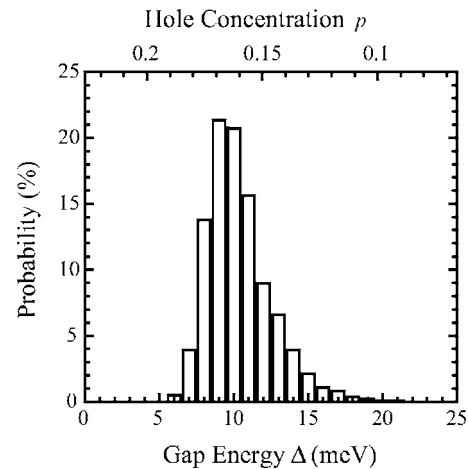


FIG. 4. Histogram of Δ obtained from the STS results shown in Fig. 3(a). The local hole concentration p evaluated from the Δ - p relation was shown in the upper axis (see the text).

Δ to increase as p decreases in HTS.^{20,25,26} By adopting the Δ - p relation by Nakano *et al.*,²⁰ p was evaluated from gap energy Δ and shown in the upper axis in Fig. 4. In this scale, p ranges from 0.12 to 0.18. The value of $p_{\text{mean}} \approx 0.16$, corresponding to $\Delta_{\text{mean}} = 10.3 \text{ meV}$, is consistent with the bulk Sr concentration of our sample. No additional peak at a particular p value, such as $p = 1/8$, has been observed.

Singer *et al.* reported the temperature dependence of the spatial variation of p in LSCO by ^{63}Cu NQR could be deduced from the frequency dependence of the $1/T_1$ curves.¹⁵ They obtained that the extent of the p variation was about 0.06 in the $x=0.16$ sample below 100 K . This value agrees with our STS results, and the “patch” size of about 6 nm in diameter estimated by their experiments is also close to our real space observation. Therefore, we believe that the inhomogeneity observed by our STS measurement is the same entity as that observed by NQR. This agreement indicates that our STS results reflect a bulk nature not peculiar to the surface.

The length scale of the spatial variation of Δ is also comparable to the correlation length of the incommensurate peaks at 8 K observed by the neutron scattering experiments.²⁷ This suggests that the dynamic fluctuation of charge and spin observed by the neutron scattering is affected by the local static structure: the fluctuation is disturbed by the static inhomogeneity in the length scale of $5\text{--}10 \text{ nm}$ and shows the disordered nature.

Our real space observation in LSCO has revealed the existence of a static distribution in the electronic states similar to that observed in Bi2212. The inhomogeneity is thought to be a common characteristic among the cuprates. Nevertheless, there is a difference between them. In Bi2212, the region where the tunneling spectra show the pseudogaplike characteristics without apparent coherence peaks is regarded as the “nonsuperconducting region”.¹¹ In LSCO, over 70% of the spectra have no apparent coherence peaks, and the magnitude of the observed peaks (if they exist) is weaker than that in Bi2212, as seen in Figs. 2 and 3(b). By applying the Δ - p relation to all spectra, regardless of the appearance of the coherence peaks, we obtained the symmetrical distri-

bution of p around the bulk Sr concentration and found an agreement with the bulk measurements. Thus, the spectrum without apparent coherence peaks is believed to represent superconducting states. Therefore, in LSCO the appearance of coherence peaks in the tunneling spectra does not seem to provide a good criterion for considering whether or not the region where the spectra were obtained is superconducting or nonsuperconducting. The relationship between these spectra and the pseudogap is crucial, although the pseudogap state in LSCO has not been well studied with high energy resolution. Further study of the pseudogap state in the underdoped LSCO with a tunneling technique is needed.

In conclusion, we have succeeded in the first STM/STS measurements on an optimally doped LSCO single crystal. The surface topography and the spatial distribution of the electronic states have been obtained. The presence of the static electronic inhomogeneity has been demonstrated in real space and it is in agreement with the bulk measurements. The inhomogeneous electronic states seem to be a common characteristic of HTS, although there are a few differences between La- and Bi-based materials. This observation is also crucial for considering further studies of the vortices in the magnetic fields or the static stripe order in La-based materials, such as $\text{La}_{2-x-y}\text{Nd}_y\text{Sr}_x\text{CuO}_4$.²⁸

*Electronic address: j1203702@rs.kagu.tus.ac.jp

- ¹S. H. Pan, E. W. Hudson, K. M. Lang, H. Eisaki, S. Uchida, and J. C. Davis, *Nature (London)* **403**, 746 (2000).
- ²E. W. Hudson, K. M. Lang, V. Madhavan, S. H. Pan, H. Eisaki, S. Uchida, and J. C. Davis, *Nature (London)* **411**, 920 (2001).
- ³H. F. Hess, R. B. Robinson, and J. V. Waszczak, *Phys. Rev. Lett.* **64**, 2711 (1990).
- ⁴H. Sakata, M. Oosawa, K. Matsuba, N. Nishida, H. Takeya, and K. Hirata, *Phys. Rev. Lett.* **84**, 1583 (2000).
- ⁵H. Sakata, N. Nishida, M. Hedo, K. Sakurai, Y. Inada, Y. Ōnuki, E. Yamamoto, and Y. Haga, *J. Phys. Soc. Jpn.* **69**, 1970 (2000).
- ⁶I. Maggio-Aprile, Ch. Renner, A. Erb, E. Walker and Ø. Fischer, *Phys. Rev. Lett.* **75**, 2754 (1995).
- ⁷Ch. Renner, B. Revaz, K. Kadowaki, I. Maggio-Aprile and Ø. Fischer, *Phys. Rev. Lett.* **80**, 3606 (1998).
- ⁸S. H. Pan, E. W. Hudson, A. K. Gupta, K.-W. Ng, H. Eisaki, S. Uchida, and J. C. Davis, *Phys. Rev. Lett.* **85**, 1536 (2000).
- ⁹J. E. Hoffman, E. W. Hudson, K. M. Lang, V. Madhavan, H. Eisaki, S. Uchida, and J. C. Davis, *Science* **295**, 466 (2002).
- ¹⁰S. H. Pan, J. P. O'Neal, R. L. Badzey, C. Chamon, H. Ding, J. R. Engelbrecht, Z. Wang, H. Eisaki, S. Uchida, A. K. Gupta, K.-W. Ng, E. W. Hudson, K. M. Lang, and J. C. Davis, *Nature (London)* **413**, 282 (2001).
- ¹¹K. M. Lang, V. Madhavan, J. E. Hoffman, E. W. Hudson, H. Eisaki, S. Uchida, and J. C. Davis, *Nature (London)* **415**, 412 (2002).
- ¹²C. Howald, H. Eisaki, N. Kaneko, M. Greven, and A. Kapitulnik, *Phys. Rev. B* **67**, 014533 (2003).
- ¹³J. W. Loram, J. L. Tallon, and W. Y. Liang, *Phys. Rev. B* **69**, 060502(R) (2004).
- ¹⁴B. W. Hoogenboom, K. Kadowaki, B. Revaz and Ø. Fischer, *Physica C* **391**, 376 (2003).
- ¹⁵P. M. Singer, A. W. Hunt, and T. Imai, *Phys. Rev. Lett.* **88**, 047602 (2002).
- ¹⁶S. V. Dordevic, S. Komiya, Y. Ando, and D. N. Basov, *Phys. Rev. Lett.* **91**, 167401 (2003).
- ¹⁷E. S. Božin, G. H. Kwei, H. Takagi, and S. J. L. Billinge, *Phys. Rev. Lett.* **84**, 5856 (2000).
- ¹⁸J. R. Kirtley, C. C. Tsuei, S. I. Park, C. C. Chi, J. Rozen, and M. W. Shafer, *Phys. Rev. B* **35**, 7216 (1987).
- ¹⁹S. Pan, K. W. Ng, A. L. de Lozanne, J. M. Tarascon, and L. H. Greene, *Phys. Rev. B* **35**, 7220 (1987).
- ²⁰T. Nakano, N. Momono, M. Oda, and M. Ido, *J. Phys. Soc. Jpn.* **67**, 2622 (1998).
- ²¹T. Kato, H. Morimoto, A. Katagiri, S. Okitsu, and H. Sakata, *Physica C* **392–396**, 221 (2003).
- ²²I. Tanaka, K. Yamane, and H. Kojima, *J. Cryst. Growth* **96**, 711 (1989).
- ²³R. Matzdorf, Z. Fang, Ismail, J. Zhang, T. Kimura, Y. Tokura, K. Terakura, and E. W. Plummer, *Science* **289**, 746 (2000).
- ²⁴Q. Li, M. Suenaga, T. Kimura, and K. Kishio, *Phys. Rev. B* **47**, 11384 (1993).
- ²⁵A. Ino, C. Kim, M. Nakamura, T. Yoshida, T. Mizokawa, A. Fujimori, Z.-X. Shen, T. Kakeshita, H. Eisaki, and S. Uchida, *Phys. Rev. B* **65**, 094504 (2002).
- ²⁶N. Miyakawa, P. Guptasarma, J. F. Zasadzinski, D. G. Hinks, and K. E. Gray, *Phys. Rev. Lett.* **80**, 157 (1998).
- ²⁷K. Yamada, C. H. Lee, K. Kurahashi, J. Wada, S. Wakimoto, S. Ueki, H. Kimura, Y. Endoh, S. Hosoya, G. Shirane, R. J. Birge-neau, M. Greven, M. A. Kastner, and Y. J. Kim, *Phys. Rev. B* **57**, 6165 (1998).
- ²⁸J. M. Tranquada, B. J. Sternlieb, J. D. Axe, Y. Nakamura, and S. Uchida, *Nature (London)* **375**, 561 (1995).